

# Feature Selection using Sparse Adaptive Bottleneck Centroid-Encoder

**Tomojit Ghosh**

*Department of Mathematics  
Colorado State University  
Fort Collins, CO 80523, USA*

TOMOJIT.GHOSH@COLOSTATE.EDU

**Michael Kirby**

*Department of Mathematics  
Colorado State University  
Fort Collins, CO 80523, USA*

KIRBY@MATH.COLOSTATE.EDU

**Editor:** TBD

## Abstract

We introduce a novel nonlinear model, Sparse Adaptive Bottleneck Centroid-Encoder (SABCE), for determining the features that discriminate between two or more classes. The algorithm aims to extract discriminatory features in groups while reconstructing the class centroids in the ambient space and simultaneously use additional penalty terms in the bottleneck layer to decrease within-class scatter and increase the separation of different class centroids. The model has a sparsity-promoting layer (SPL) with a one-to-one connection to the input layer. Along with the primary objective, we minimize the  $l_{2,1}$ -norm of the sparse layer, which filters out unnecessary features from input data. During training, we update class centroids by taking the Hadamard product of the centroids and weights of the sparse layer, thus ignoring the irrelevant features from the target. Therefore the proposed method learns to reconstruct the critical components of class centroids rather than the whole centroids. The algorithm is applied to various real-world data sets, including high-dimensional biological, image, speech, and accelerometer sensor data. We compared our method to different state-of-the-art feature selection techniques, including supervised Concrete Autoencoders (SCAE), Feature Selection Networks (FsNet), Stochastic Gates (STG), and LassoNet. We empirically showed that SABCE features often produced better classification accuracy than other methods on the sequester test sets, setting new state-of-the-art results.

## 1. Introduction

Technological advancement has made high-dimensional data readily available. For example, in bioinformatics, the researchers seek to understand the gene expression level with microarray or next-generation sequencing techniques where each point consists of over 50,000 measurements (Pease et al., 1994; Shalon et al., 1996; Metzker, 2010; Reuter et al., 2015). The abundance of features demands the development of feature selection algorithms to improve a Machine Learning task, e.g., classification. Another important aspect of feature selection is knowledge discovery from data. Which biomarkers are important to characterize a biological process, e.g., the immune response to infection by respiratory viruses such as

influenza (O’Hara et al., 2013)? Additional benefits of feature selection include improved visualization and understanding of data, reducing storage requirements, and faster algorithm training times.

Feature selection can be accomplished in various ways that can be broadly categorized as filter, wrapper, and embedded methods. In a filter method, each variable is ordered based on a score. After that, a threshold is used to select the relevant features (Lazar et al., 2012). Variables are usually ranked using correlation (Guyon and Elisseeff, 2003; Yu and Liu, 2003), and mutual information (Vergara and Estévez, 2014; Fleuret, 2004). In contrast, a wrapper method uses a model and determines the importance of a feature or a group of features by the generalization performance of the predetermined model (El Aboudi and Benhlima, 2016; Hsu et al., 2002). Since evaluating every possible combination of features becomes an NP-hard problem, heuristics are used to find a subset of features. Wrapper methods are computationally intensive for larger data sets, in which case search techniques like Genetic Algorithm (GA) (Goldberg and Holland, 1988) or Particle Swarm Optimization (PSO) (Kennedy and Eberhart, 1995) are used. In embedded methods, feature selection criteria are incorporated within the model, i.e., the variables are picked during the training process (Lal et al., 2006). Iterative Feature Removal (IFR) uses the ratio of absolute weights of a Sparse SVM model as a criterion to extract features from the high dimensional biological data set (O’Hara et al., 2013).

Mathematically feature selection problem can be posed as an optimization problem on  $\ell_0$ -norm, i.e., how many predictors are required for a machine learning task. As the minimization of  $\ell_0$  is intractable (non-convex and non-differentiable),  $\ell_1$ -norm is used instead, which is a convex proxy of  $\ell_0$  (Tibshirani, 1996). Although the  $\ell_1$  has been used in the feature selection task in linear (Fonti and Belitser, 2017; Muthukrishnan and Rohini, 2016; Kim and Kim, 2004; O’Hara et al., 2013; Chepushtanova et al., 2014) as well as in nonlinear regime (Li et al., 2016; Scardapane et al., 2017; Li et al., 2020), it has some disadvantages as well. For example, when multi-collinearity exists (i.e., two or more independent features have a high correlation with one another) in data,  $\ell_1$  selects one of them and discards the rest, degrading the rest prediction performance (Zou and Hastie, 2005). Although the problem can be overcome using iterative feature removal scheme as proposed by (O’Hara et al., 2013). It has been reported that minimizing Lasso doesn’t satisfy the Oracle property (Zou, 2006). ElasticNet (Zou and Hastie, 2005), on the other hand, overcomes some limitations of Lasso by combining  $\ell_2$  norm with  $\ell_1$ -norm.

This paper proposes a new embedded variable selection approach called Sparse Adaptive Bottleneck Centroid-Encoder (SABCE) to extract features when class labels are available. Our method modifies the Centroid-Encoder model (Ghosh et al., 2018; Ghosh and Kirby, 2022) by incorporating two penalty terms in the bottleneck layer to increase class separation and localization. SABCE applies a  $\ell_{2,1}$  penalty to a sparsity-promoting layer between the input and the first hidden layer while reconstructing the class centroids. One key attribute of SABCE is the adaptive centroids update during training, distinguishing it from Centroid-Encoder, which has a fixed class centroid. We evaluate the proposed model on diverse data sets and show that the features produce better generalization than other state-of-the-art techniques.

## 2. Sparse Adaptive Bottleneck Centroid-Encoder (SABCE)

Consider a data set  $X = \{x_i\}_{i=1}^N$  with  $N$  samples and  $M$  classes where  $x_i \in \mathbb{R}^d$ . The classes denoted  $C_j, j = 1, \dots, M$  where the indices of the data associated with class  $C_j$  are denoted  $I_j$ . We define centroid of each class as  $c_j = \frac{1}{|C_j|} \sum_{i \in I_j} x_i$  where  $|C_j|$  is the cardinality of class  $C_j$ .

### 2.1 Bottleneck Centroid-Encoder (BCE)

Given the setup mentioned above, we define Bottleneck Centroid-Encoder, which is the starting point of our proposed algorithm. The objective function of BCE is given below:

$$\mathcal{L}_{bce}(\theta) = \frac{1}{2N} \sum_{j=1}^M \sum_{i \in I_j} (\|c_j - f(x_i; \theta)\|_2^2 + \mu_1 \|g(c_j) - g(x_i)\|_2^2) + \mu_2 \sum_{k < l} \frac{1}{1 + \|g(c_k) - g(c_l)\|_2^2} \quad (1)$$

The mapping  $f$  is composed of a dimension-reducing mapping  $g$  (encoder) followed by a dimension-increasing reconstruction mapping  $h$  (decoder). The first term of the objective is minimizing the square of the distance between  $f(x_i)$  and its class centroid  $c_j$ . Therefore the aim is to map the sample  $x_i$  to its corresponding class centroid  $c_j$ , and the mapping function  $f$  is known as Centroid-Encoder (Ghosh and Kirby, 2022). The output of the encoder  $g$  is used as a supervised visualization tool (Ghosh and Kirby, 2022; Ghosh et al., 2018). Centroid-Encoder calculates its cost on the output layer; if the centroids of multiple classes are close in ambient space, the corresponding samples will land close in the reduced space, increasing the error rate. To remedy the situation, we add two more terms to the bottleneck layer, i.e., at the output of the encoder  $g$ , which we call Bottleneck Centroid-Encoder (BCE). The term  $\|g(c_j) - g(x_i)\|_2^2$  will further pull a sample  $x_i$  towards its centroid which will improve the class localization in reduced space. Further, to avoid the overlap of classes in the latent bottleneck space, we introduce a term that serves to repel centroids there. We achieve this by maximizing the distances (equivalently the square of the  $\ell_2$ -norm) between all class-pairs of latent centroids. We introduced the third term to fulfill the purpose. Note, as the original optimization is a minimization problem, we choose to minimize  $\sum_{k < l} \frac{1}{1 + \|g(c_k) - g(c_l)\|_2^2}$  which will ultimately increase the distance between the latent centroids of class  $k$  and  $l$ . We added 1 in the denominator for numerical stability. The hyper parameters  $\mu_1$  and  $\mu_2$  will control the class localization and separation in the embedded space. We use a validation set to determine their values.

### 2.2 Sparse Adaptive Bottleneck Centroid-Encoder for Robust Feature Selection

The Sparse Bottleneck Centroid-Encoder (SBCE) is a modification to the BCE architecture as shown in Figure 1. The input layer is connected to the first hidden layer via the sparsity promoting layer (SPL). Each node of the input layer has a weighted one-to-one connection to each node of the SPL. The number of nodes in these two layers are the same. The nodes in SPL don't have any bias or non-linearity. The SPL is fully connected to the first hidden layer, therefore the weighted input from the SPL will be passed to the hidden layer in the same way that of a standard feed forward network. During training, an  $\ell_{2,1}$  penalty, which is

also known as Elastic Net (Zou and Hastie, 2005), will be applied to the weights connecting the input layer and SPL layer. The sparsity promoting  $\ell_{2,1}$  penalty will drive most of the weights to near zero and the corresponding input nodes/features can be discarded. Therefore, the purpose of the SPL is to select important features from the original input. Note we only apply the  $\ell_{2,1}$  penalty to the parameters of the SPL.

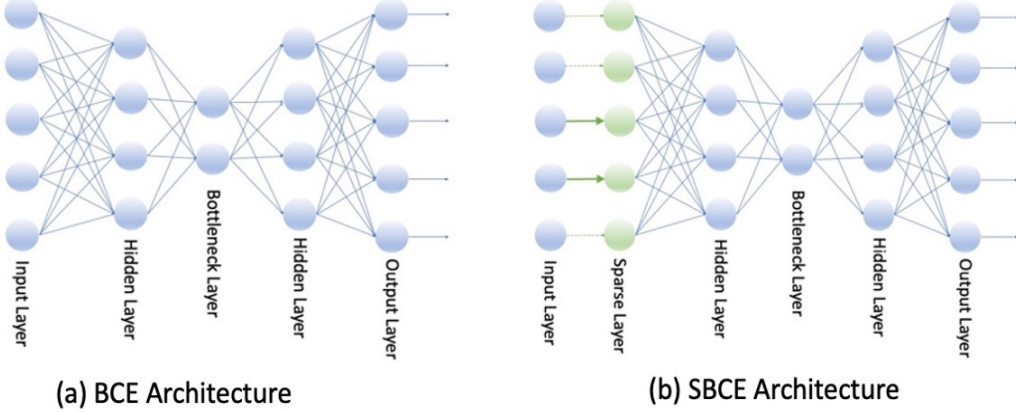


Figure 1: The architecture of Bottleneck Centroid-Encoder and Sparse Bottleneck Centroid-Encoder. Notice that Sparse Bottleneck Centroid-Encoder employs a sparse layer between the input and the first hidden layer to promote feature sparsity using  $\ell_{2,1}$  norm.

Denote  $\theta_{spl}$  to be the parameters (weights) of the SPL and  $\theta$  to be the parameters of the rest of the network. The cost function of sparse bottleneck centroid-encoder is given by

$$\begin{aligned} \mathcal{L}_{sbce}(\theta, \theta_{spl}) = & \frac{1}{2N} \sum_{j=1}^M \sum_{i \in I_j} (\|c_j - f(x_i; \theta)\|_2^2 + \mu_1 \|g(c_j) - g(x_i)\|_2^2) \\ & + \mu_2 \sum_{k < l} \frac{1}{1 + \|g(c_k) - g(c_l)\|_2^2} + \lambda_1 \|\theta_{spl}\|_1 + \lambda_2 \|\theta_{spl}\|_2^2 \end{aligned} \quad (2)$$

where  $\lambda_1, \lambda_2$  are the hyperparameter which control the sparsity. A larger value of  $\lambda_1$  will promote higher sparsity resulting more near-zero weights in SPL.

### 2.2.1 SPARSIFICATION OF THE CENTROIDS

The targets of the SBCE are the class centroids which are pre-computed from data and labels. For high-dimensional datasets, the features are noisy, redundant, or irrelevant (Alelyani et al., 2018); therefore, feature selection with fixed class centroids, computed on high-dimensional ambient space, may be impacted by the noise. We can remedy the situation by promoting sparsity in the class centroid during training. In this approach, we start with  $c_j$ 's computed in the ambient space; after that, we change  $c_j$ 's by multiplying it component-wise by  $\theta_{spl}$ , i.e.,  $[c_j]_t = [c_j] \odot [\theta_{spl}]_{t-1}$ , where  $t$  is the current epoch. As  $\theta_{spl}$  sparsifies the input data by eliminating redundant and noisy features, updating the centroids as shown above will reduce noise from the targets, thus improving the discriminative power of selected features. We call this algorithm as Sparse Adaptive Bottleneck Centroid-Encoder

(SABCE). In Equation 2, we use  $[c_j]_t$  (instead of  $c_j$ ) to calculate the cost at each iteration. The comparison in Table 1 shows the performance advantage of SABCE over SBCE.

Models	Data set				
	Mice Protein	MNIST	FMNIST	GLIOMA	Prostate_GE
SBCE	95.8	92.5	85.0	65.6	88.2
SABCE	<b>99.8</b>	<b>94.0</b>	<b>85.4</b>	<b>74.2</b>	<b>90.2</b>

Table 1: Comparison between SBCE and SABCE on five benchmarking data sets using top 50 features. We use the same network architecture and hyper parameters in training. We follow the same experimental set up as in Section 3.

**Training Details:** We implemented SLCE in PyTorch (Paszke et al., 2017) to run on GPUs on Tesla V100 GPU machines. We trained SABCE using Adam (Kingma and Ba, 2015) on the whole training set without minibatch. We pre-train our model for ten epochs and then include the sparse layer (SPL) with the weights initialized to 1. Then we train the model for another ten epochs to adjust the weights of the SPL. After that, we did an end-to-end training applying  $\ell_{2,1}$ -penalty on the SPL for 1000 epochs. Like any neural network-based model, the hyperparameters of SABCE need to be tuned for optimum performance. Table 2 contains the list with the range of values we used in this paper. We used validation set to choose the optimal value. Section A of Appendix has information on reproducibility. We will provide the code with a dataset as supplementary material.

Hyper parameter	Range of Values
# Hidden Layers (L)	{1, 2}
# Hidden Nodes (H)	{50,100,200,250,500}
Activation Function	Hyperbolic tangent (tanh)
$\mu_1, \mu_2$	{0.1, 0.2, 0.3, 0.4, 0.5, 0.6, 0.7}
$\lambda_1, \lambda_2$	{0.01, 0.001, 0.0001, 0.0002, 0.0004, 0.0006, 0.0008}

Table 2: Hyperparameters for Sparse Adaptive Bottleneck Centroid-Encoder.

### 2.2.2 FEATURE CUT-OFF

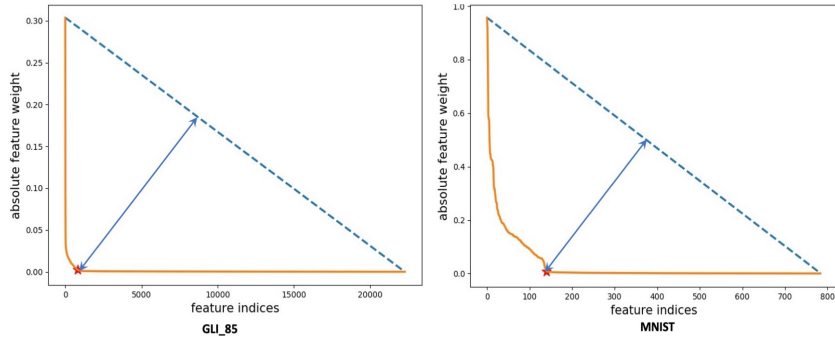


Figure 2: Feature selection cut off geometry.

As shown in Figure 2, the  $\ell_{2,1}$ -norm of the sparse layer (SPL) drives a lot of weights to near zero. Often hard thresholding or a ratio of two consecutive weights is used to pick the nonzero weight (O’Hara et al., 2013).

In this article, we take a different approach to select the set of discriminatory features as shown in Figure 2. After training SBCE, we arrange the absolute value of the weights of the sparse layer in descending order forming a curve (the orange one). We then join the first and the last point of the curve with a straight line (the blue dotted line). We measure the distance of each point on the curve to the straight line. The point with the largest distance is the position (P) of the elbow. We pick all the features whose absolute weight is greater than that of P. Figure 2 demonstrates the approach on GLL85 and MNIST set. The red star indicates the position of point P (the elbow), and the absolute weight of features on the left of P is higher than on the right, selecting only 796 out of 22,283 features from GLL85 and 137 out of 784 MNIST pixels.

### 2.3 Empirical Analysis of SBCE

In this section we present a series of analyses of the proposed model to understand its behavior.

**1. Analysis of Hyper-parameters  $\mu_1$  and  $\mu_2$ :** The hyper-parameters  $\mu_1$  and  $\mu_2$  control the class scatter and separation in bottleneck space. We ran an experiment on the MNIST digits to understand the effect of  $\mu_1$  and  $\mu_2$  on model’s performance. We put aside 20% of samples from each class as a validation set and the rest of the data set is used to train the model for each combination of  $\mu_1$  and  $\mu_2$ . The validation set is used to compute the error rate using a 5-NN classifier in the two-dimensional space. Figure 3 shows the errors for different combinations of  $\mu_1$  and  $\mu_2$  in a heat map. Observe that the error rate increases

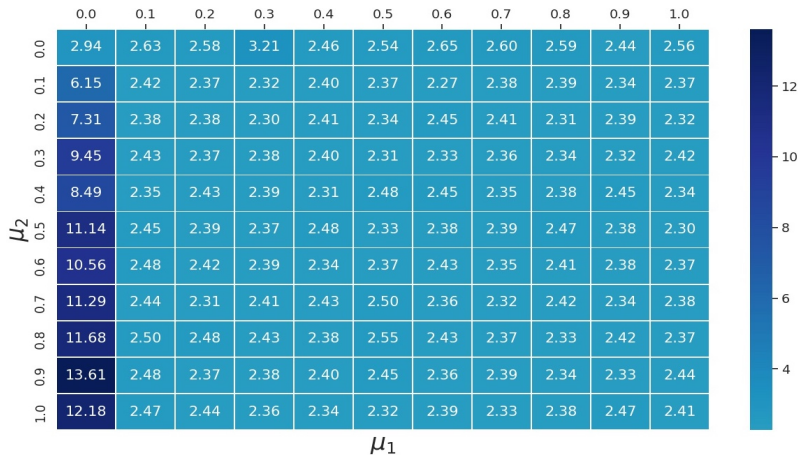


Figure 3: Analysis of error rate with changes to  $\mu_1$  and  $\mu_2$ .

with  $\mu_2$  when  $\mu_1$  is zero. The behavior is not surprising as setting  $\mu_1$  to zero nullifies the effect of the second term (see Equation 2), which would hold the samples tightly around their centroid in reduced space. The gradient from the first term will exert a pulling force to bind the samples around their centroids, but the gradient coming from the third term will dominate the gradient of the first term as  $\mu_2$  increases. As an effect, the class-scatter increases in low dimensional space resulting in misclassifications. As soon as  $\mu_1$  increases

to 0.1, the error rate decreases significantly. After that, a higher value of  $\mu_2$  doesn't change the results too much. The minimum validation error occurs for  $\mu_1 = 0.6$  and  $\mu_2 = 0.1$ . The analysis reveals that  $\mu_1$  is relatively more important than  $\mu_2$ .

**2. Analysis of Feature Sparsity:** Here, we study sparsity promotion on six represen-

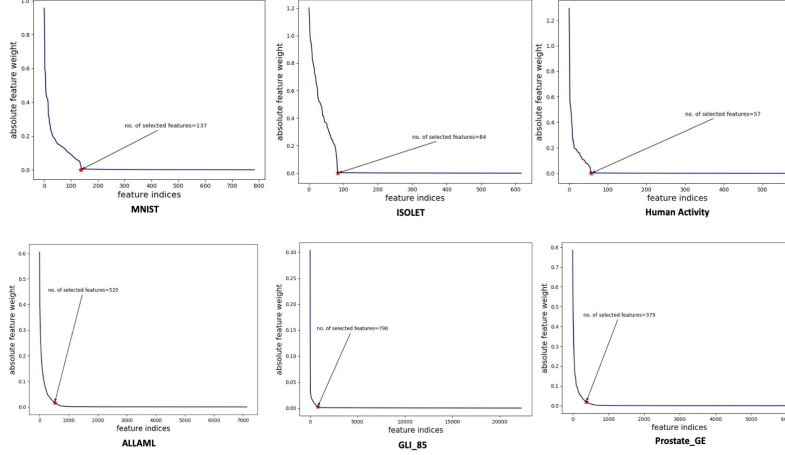
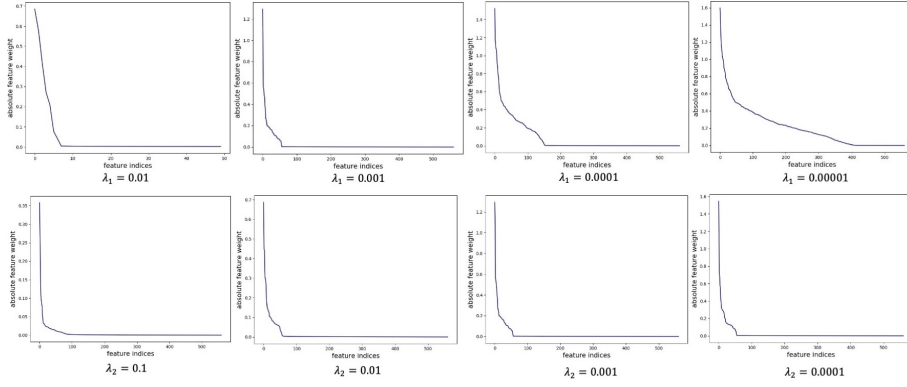


Figure 4: Sparsity analysis of SABCE on six data sets. MNIST, ISOLET, and Human Activity have more samples than features while ALLAML, GLI\_85, and Prostate\_GE have more features than data points; see Table 3 for more details. In each case, we plotted the absolute value of weights of the sparse layer in descending order. In all the experiments, we set  $\lambda_1, \lambda_2$ , to 0.001. These plots suggest the model promotes sparsity, driving most of the weights in the sparsity layer to near zero.

tative data sets. Three datasets contain more samples than features: MNIST, ISOLET, and Human Activity. These data sets are also from different domains, namely image, speech, and accelerometer sensors. We also use three biological data sets: ALLAML, GLI\_85, and Prostate\_GE, where the sample size is significantly smaller when compared to the number of features (see Table 3). We fit our model on the training partition of each data set and then plot the absolute value of the weights of the sparse layer in descending order as shown in Figure 4. As can be seen, the model promotes sparsity in each case, driving most of the weights in the sparse layer to near zero ( $10^{-4}$  to  $10^{-6}$ ). The rest of the features have significantly higher values, and our feature cut-off technique distinguishes them successfully, pointing out the number of selected features in each case.

**3. Effect of  $\lambda_1$  and  $\lambda_2$  on Feature Sparsity:** In Figure 5, we show how hyper-parameters  $\lambda_1$  and  $\lambda_2$  control sparsity on Human Activity data. We fix  $\lambda_2$  to 0.001 and run SABCE with different values of  $\lambda_1$ , which we show in the first row. Observe that the solution become less sparse with the decrease of  $\lambda_1$ . In the second row, we present a similar plot over different values of  $\lambda_2$  while fixing  $\lambda_1$  to 0.001. The change of  $\lambda_2$  doesn't contribute too much to the model's sparsity.

Figure 5: Effect of  $\lambda_1$  and  $\lambda_2$  on sparsity.

**4. Generalization Property of Selected Features:** To investigate the generalization aspect of the features, we restrict training and validation sets to the selected variables. We fit a one-hidden layer neural network on the training set to predict the class label of the validation samples. Figure 6 shows the accuracy as a function of feature count.

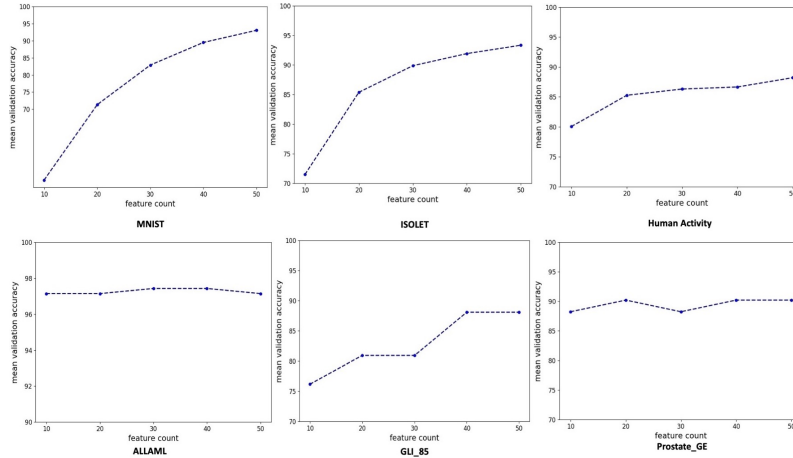


Figure 6: Accuracy on the validation set as a function of the number of features.

The plot suggests that the selected features can accurately predict unseen samples. We see that the accuracy increases with the number of features for MNIST, ISOLET Human Activity, and GLL85; in contrast, adding more features does not change the accuracy for ALLAML and Prostate\_GE significantly.

**5. Feature Selection Stability:** In this experiment, we shed light on the stability of the feature selection process; specifically, we want to compare and contrast the feature sets across several trials. To this end, We run our model five times on two high-dimensional biological data, ALLAML, Prostate\_GE, and one high sample size data Human Activity and then compare the feature sets.

Figure 7 shows the results using Venn diagrams. Observe that the number of selected features over five runs are generally close to each other. In each case, there is a significant number of overlapping features. For each data set, we calculate the Jaccard index using the five feature sets to measure their similarity—the Jaccard index of ALLAML, Prostate\_GE,



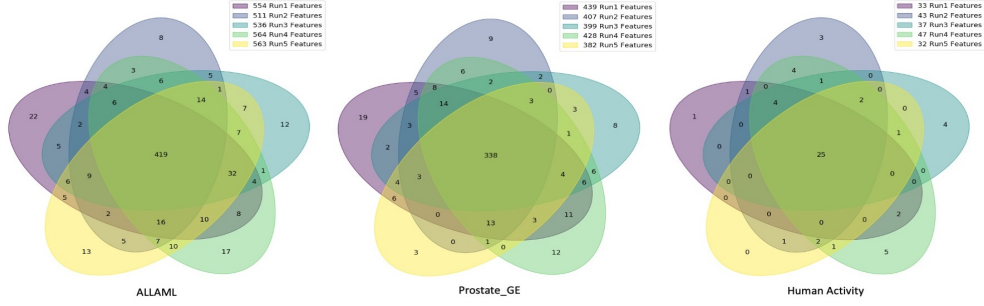


Figure 7: Venn diagram of five sets of features for each of the three high-dimensional data sets.

and Human Activity are 0.6254, 0.6828, and 0.6253, respectively. High Jaccard scores indicate that the feature sets have a lot of commonality over different runs.

### 3. Experimental Results

We present the comparative evaluation of our model on various data sets using several feature selection techniques.

#### 3.1 Experimental Details

Dataset	No. Features	No. of Classes	No. of Samples	Domain
ALLAML	7129	2	72	Biology
GLIOMA	4434	4	50	Biology
SMK_CAN	19993	2	187	Biology
Prostate_GE	5966	2	102	Biology
GLI.85	22283	2	85	Biology
CLL.SUB	11340	3	111	Biology
Mice Protein	77	8	975	Biology
COIL20	1024	20	1440	Image
Isolet	617	26	7797	Speech
Human Activity	561	6	5744	Accelerometer Sensor
MNIST	784	10	70000	Image
FMNIST	784	10	70000	Image

Table 3: Descriptions of the data sets used for benchmarking experiments.

We used twelve data sets from a variety of domains (image, biology, speech, and sensor; see Table 3) and five neural network-based models to run three benchmarking experiments. To this end, we picked the published results from two papers (Lemhadri et al., 2021; Singh et al., 2020) for benchmarking and we ran the Stochastic Gate (Yamada et al., 2020) using the code provided by authors. We followed the same experimental methodology described in (Lemhadri et al., 2021; Singh et al., 2020) for an apples-to-apples comparison. This approach permitted a direct comparison of LassoNet, FsNet, Supervised CAE using the authors’ best results. All three experiments follow the standard workflow:

- Split each data sets into training and test partition.
- Run SABCE on the training set to extract top  $K \in \{10, 50\}$  features.
- Using the top  $K$  features train a one hidden layer ANN classifier with  $H$  ReLU units to predict the test samples. The  $H$  is picked using a validation set.
- Repeat the classification 20 times and report average accuracy.

Now we describe the details of the two experiments.

**Experiment 1:** The first bench-marking experiment is conducted on six publicly available (Li et al., 2018) high dimensional biological data sets: ALLAML, GLIOMA, SMK\_CAN, Prostate\_GE, GLI.85, and CLL\_SUB<sup>1</sup> to compare SABCE with FsNet, Supervised CAE (SCAE), and Stochastic Gates (STG). Following the experimental protocol of Singh et al. (Singh et al., 2020), we randomly partitioned each data into a 50:50 ratio of train and test and ran SABCE, STG on the training set. After that, we calculated the test accuracy using the top  $K = \{10, 50\}$  features. We repeated the experiment 20 times and reported the mean accuracy. We ran a 5-fold cross-validation on the training set to tune the hyperparameters.

**Experiment 2:** In the second bench-marking experiment, we compared our approach with LassoNet(Lemhadri et al., 2021) and Stochastic Gate(Yamada et al., 2020) on six data sets: Mice Protein<sup>2</sup>, COIL20, Isolet, Human Activity, MNIST, and FMNIST<sup>3</sup>. Following the experimental set of Lemhadri et al., we split each data set into 70:10:20 ratio of training, validation, and test sets. We ran SCE on the training set to pick the top  $K = 50$  features to predict the class labels of the sequester test set. We extensively used the validation set to tune the hyperparameters.

### 3.2 Results

Now we discuss the results of the benchmarking experiments. In Table 4 we present the results of the first experiment where we compare SABCE, SCAE, STG, and FsNet on six high-dimensional biological data sets. Apart from the results using a subset (10 and 50) of features, we also provide the prediction using all the features. In most cases, feature selection helps improve classification performance. Generally, SABCE features perform better than SCAE and FsNet; out of the twelve classification tasks, SABCE produces the best result on ten. Notice that the top fifty SABCE features give a better prediction rate than the top ten in all the cases. Interestingly, the accuracy of SCAE and FsNet drop significantly on SMK\_CAN, GLI.85 and CLL\_SUB using the top fifty features.

Now we turn our attention to the results of the second experiment, as shown in Table 5. The features of the SABCE produce better classification accuracy than LassoNet in all cases. Besides COIL20, our model has better accuracy by a margin of 4% – 6.5%. On the other hand, STG performed slightly better (a margin of 0.4% to 0.7%) than SABCE on Mice Protein, COIL20, and MNIST. In contrast, our model is more accurate than STG

---

1. Available at <https://jundongl.github.io/scikit-feature/datasets.html>  
 2. There are some missing entries that are imputed by mean feature values.  
 3. Available at UCI Machine Learning repository

Data set	Top 10 features				Top 50 features				All Fea.
	FsNet	SCAE	STG	SABCE	FsNet	SCAE	STG	SABCE	
ALLAML	91.1	83.3	81.0	<b>93.7</b>	92.2	93.6	88.5	<b>94.6</b>	89.9
Prostate_GE	87.1	83.5	82.3	<b>89.9</b>	87.8	88.4	85.0	<b>90.1</b>	75.9
GLIOMA	62.4	58.4	62.0	<b>66.8</b>	62.4	60.4	70.4	<b>74.2</b>	70.3
SMK_CAN	<b>69.5</b>	68.0	65.2	68.1	64.1	66.7	68.0	<b>69.4</b>	65.7
GLI_85	87.4	<b>88.4</b>	72.2	84.7	79.5	82.2	81.0	<b>85.7</b>	79.5
CLL_SUB	64.0	57.5	54.4	<b>70.8</b>	58.2	55.6	63.2	<b>72.2</b>	56.9

Table 4: Comparison of mean classification accuracy of FsNet, SCAE, STG and SABCE features on six real-world high-dimensional biological data sets. The prediction rates are averaged over twenty runs on the test set. Numbers for FsNet and SCAE are being reported from (Singh et al., 2020). The last column reports accuracy using all features using an ANN classifier.

on FMNIST, ISOLET, and Activity by 1.6% to 4.2%. Note that LassoNet is the worst-performing model. In this experiment, STG performed competitively compared to the first, where STG’s performance was significantly worse than that of SABCE. Upon further investigation, it turns out that the model fails to induce feature sparsity on all six high-dimensional biological data sets. We fit the model on the training partition of each data set and then plot the probability of the stochastic gates in descending order, which we call the *sparsity plot*. We run STG using a wide range on  $\lambda$ , which controls the sparsity of the model. In Figure 8, we show the result on ALLAML data. As we can see, the model doesn’t create a sparse solution for input features for any of the nine values. Ideally, we should have observed the probability of many variables to near zero so that those features could be ignored. Changing the activation function, number of hidden nodes, or depth of the network doesn’t produce a sparser solution. We kept the similar analysis on other data sets in Appendix (Section C).

Data set	Top 50 features			All features ANN
	LassoNet	STG	SABCE	
Mice Protein	95.8	<b>99.8</b>	99.4	99.00
MNIST	87.3	<b>94.7</b>	94.0	92.8
FMNIST	80.0	83.8	<b>85.4</b>	88.30
ISOLET	88.5	90.9	<b>93.3</b>	95.30
COIL-20	99.1	<b>99.7</b>	99.3	99.60
Activity	84.9	86.6	<b>90.8</b>	85.30

Table 5: Classification results using LassoNet, STG, and SABCE features on six publicly available data sets. Numbers for LassoNet and ‘All features ANN’ are reported from (Lemhadri et al., 2021). All the reported accuracies are measured on the test set.

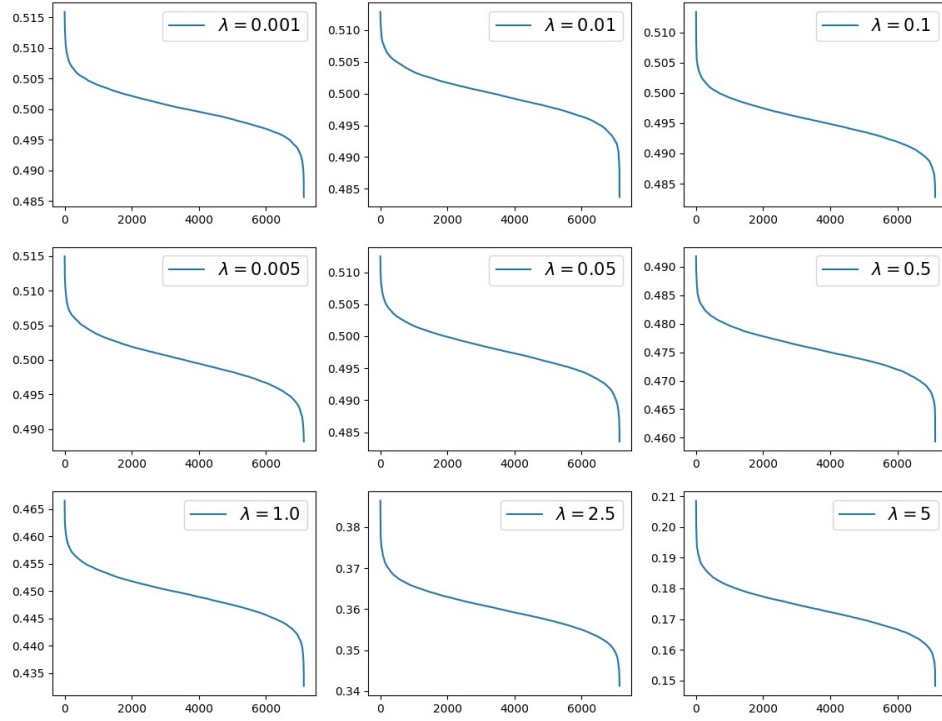


Figure 8: Sparsity analysis of Stochastic Gates on ALLAML data.

#### 4. Related Work

Feature selection has a long history spread across many fields, including bioinformatics, document classification, data mining, hyperspectral band selection, computer vision, etc. We describe the literature related to the embedded methods where the selection criteria are part of a model. The model can be either linear or non-linear. Adding an  $\ell_1$  penalty to classification and regression methods naturally produce feature selectors for linear model, see (Tibshirani, 1996; Fonti and Belitser, 2017; Muthukrishnan and Rohini, 2016; Kim and Kim, 2004; Zou and Hastie, 2005; Marafino et al., 2015; Shen et al., 2011; Sokolov et al., 2016; Lindenbaum and Steinerberger, 2021; Candes et al., 2008; Daubechies et al., 2010; Bertsimas et al., 2017; Xie and Huang, 2009). Support Vector Machines (Cortes and Vapnik, 1995) have been used extensively for feature selection, see (Marafino et al., 2015; Shen et al., 2011; Sokolov et al., 2016; Guyon et al., 2002; O’Hara et al., 2013; Chepushtanova et al., 2014).

While the linear models are generally fast and convex, they don’t capture the non-linear relationship among the input features (unless a kernel trick is applied). Non-linear models based on deep neural networks overcome these limitations. Here, we will briefly discuss a handful of such models. Group Sparse ANN (Scardapane et al., 2017) used group Lasso (Tibshirani, 1996) to impose the sparsity on a group of variables instead of a single variable. Li et al. proposed deep feature selection (DFS), which is a multilayer neural network-based feature selection technique (Li et al., 2016). (Kim et al., 2016) proposed a heuristics based technique to assign importance to each feature. Using the ReLU activation, (Roy et al.,

2015) provided a way to measure the contribution of an input feature towards hidden activation of next layer. (Han et al., 2018) developed an unsupervised feature selection technique based on the autoencoder architecture. (Taherkhani et al., 2018) proposed a RBM (Hinton et al., 2006; Hinton and Salakhutdinov, 2006) based feature selection model. Also see, (Balin et al., 2019; Yamada et al., 2020; Singh et al., 2020).

## 5. Discussion, Conclusion and Limitations

In this paper, we proposed a novel neural network-based feature selection technique, Sparse Adaptive Bottleneck Centroid-Encoder (SABCE). Using the basic multi-layer perceptron encoder-decoder neural network architecture, the model backpropagates the SABCE cost to a feature selection layer that filters out non-discriminating features by  $\ell_{2,1}$ -regularization. The setting allows the feature selection to be data-driven without needing prior knowledge, such as the number of features to be selected and the underlying distribution of the input features. The extensive analysis in Section 2.3 demonstrates that the  $\ell_{2,1}$ -norm induces good feature sparsity without shrinking all the variables. Unlike other methods, e.g., Stochastic Gates, our approach promotes feature sparsity for high-dimension and low-sample size biological datasets, further demonstrating the value of SABCE as a feature detector. We chose the  $\lambda_1$  and  $\lambda_2$  from the validation set from a wide range of values and saw that smaller values work better for classification. The plots with the Venn diagrams confirm the consistent and stable feature detection ability of SABCE.

The rigorous benchmarking with twelve data sets from diverse domains and four methods provides evidence that the features of SABCE produce better generalization performance than other state-of-the-art models. We compared SABCE with FsNet, mainly designed for high-dimensional biological data, and found that our proposed method outperformed it in most cases. In fact, our model produced new state-of-the-art results in ten cases out of twelve. The comparison also includes Supervised CAE, which is less accurate than SABCE. On the data sets where the number of observations is more than the number of variables, SABCE features produces better classification results than LassoNet in all six cases and better than Stochastic Gates on three data sets. The strong generalization performance, coupled with the ability to sparsify input features, establishes the value of our model as a nonlinear feature detector.

Although SABCE produces new state-of-the-art results on diverse data sets, our model won't be the right choice for the cases where class centroids make little sense, e.g., natural images. The current scope of the work doesn't allow us to investigate other optimization techniques, e.g., proximal gradient descent, trimmed Lasso, etc., which we plan to explore in the future.

## References

- Salem Alelyani, Jiliang Tang, and Huan Liu. Feature selection for clustering: A review. *Data Clustering*, pages 29–60, 2018.
- Muhammed Fatih Balin, Abubakar Abid, and James Zou. Concrete autoencoders: Differentiable feature selection and reconstruction. In *International conference on machine learning*, pages 444–453. PMLR, 2019.

- Dimitris Bertsimas, Martin S Copenhaver, and Rahul Mazumder. The trimmed lasso: Sparsity and robustness. *arXiv preprint arXiv:1708.04527*, 2017.
- Emmanuel J Candes, Michael B Wakin, and Stephen P Boyd. Enhancing sparsity by reweighted l1 minimization. *Journal of Fourier analysis and applications*, 14(5):877–905, 2008.
- Sofya Chepushtanova, Christopher Gittins, and Michael Kirby. Band selection in hyperspectral imagery using sparse support vector machines. In *Algorithms and Technologies for Multispectral, Hyperspectral, and Ultraspectral Imagery XX*, volume 9088, page 90881F. International Society for Optics and Photonics, 2014.
- Corinna Cortes and Vladimir Vapnik. Support vector machine. *Machine learning*, 20(3):273–297, 1995.
- Ingrid Daubechies, Ronald DeVore, Massimo Fornasier, and C Sinan Gunturk. Iteratively reweighted least squares minimization for sparse recovery. *Communications on Pure and Applied Mathematics: A Journal Issued by the Courant Institute of Mathematical Sciences*, 63(1):1–38, 2010.
- Naoual El Aboudi and Laila Benhlila. Review on wrapper feature selection approaches. In *2016 International Conference on Engineering & MIS (ICEMIS)*, pages 1–5. IEEE, 2016.
- François Fleuret. Fast binary feature selection with conditional mutual information. *Journal of Machine learning research*, 5(9), 2004.
- Valeria Fonti and Eduard Belitser. Feature selection using lasso. *VU Amsterdam Research Paper in Business Analytics*, 30:1–25, 2017.
- Tomojit Ghosh and Michael Kirby. Supervised dimensionality reduction and visualization using centroid-encoder. *Journal of Machine Learning Research*, 23(20):1–34, 2022.
- Tomojit Ghosh, Xiaofeng Ma, and Michael Kirby. New tools for the visualization of biological pathways. *Methods*, 132:26 – 33, 2018. ISSN 1046-2023. doi: <https://doi.org/10.1016/j.ymeth.2017.09.006>. URL <http://www.sciencedirect.com/science/article/pii/S1046202317300439>. Comparison and Visualization Methods for High-Dimensional Biological Data.
- David E Goldberg and John Henry Holland. Genetic algorithms and machine learning. *Machine Learning*, 1988.
- Isabelle Guyon and André Elisseeff. An introduction to variable and feature selection. *Journal of machine learning research*, 3(Mar):1157–1182, 2003.
- Isabelle Guyon, Jason Weston, Stephen Barnhill, and Vladimir Vapnik. Gene selection for cancer classification using support vector machines. *Machine learning*, 46(1):389–422, 2002.

- Kai Han, Yunhe Wang, Chao Zhang, Chao Li, and Chao Xu. Autoencoder inspired unsupervised feature selection. In *2018 IEEE International Conference on Acoustics, Speech and Signal Processing (ICASSP)*, pages 2941–2945. IEEE, 2018.
- Geoffrey E Hinton and Ruslan R Salakhutdinov. Reducing the dimensionality of data with neural networks. *science*, 313(5786):504–507, 2006.
- Geoffrey E. Hinton, Simon Osindero, and Yee-Whye Teh. A fast learning algorithm for deep belief nets. *Neural Comput.*, 18(7):1527–1554, July 2006. ISSN 0899-7667. doi: 10.1162/neco.2006.18.7.1527. URL <http://dx.doi.org/10.1162/neco.2006.18.7.1527>.
- Chun-Nan Hsu, Hung-Ju Huang, and Stefan Dietrich. The annigma-wrapper approach to fast feature selection for neural nets. *IEEE Transactions on Systems, Man, and Cybernetics, Part B (Cybernetics)*, 32(2):207–212, 2002.
- James Kennedy and Russell Eberhart. Particle swarm optimization. In *Proceedings of ICNN’95-international conference on neural networks*, volume 4, pages 1942–1948. IEEE, 1995.
- Seong Gon Kim, Nawanol Theera-Ampornpunt, Chih-Hao Fang, Mrudul Harwani, Ananth Grama, and Somali Chaterji. Opening up the blackbox: an interpretable deep neural network-based classifier for cell-type specific enhancer predictions. *BMC systems biology*, 10(2):243–258, 2016.
- Yongdai Kim and Jinseog Kim. Gradient lasso for feature selection. In *Proceedings of the twenty-first international conference on Machine learning*, page 60, 2004.
- Diederik P. Kingma and Jimmy Ba. Adam: A method for stochastic optimization. In Yoshua Bengio and Yann LeCun, editors, *3rd International Conference on Learning Representations, ICLR 2015, San Diego, CA, USA, May 7-9, 2015, Conference Track Proceedings*, 2015. URL <http://arxiv.org/abs/1412.6980>.
- Thomas Navin Lal, Olivier Chapelle, Jason Weston, and André Elisseeff. Embedded methods. In *Feature extraction*, pages 137–165. Springer, 2006.
- Cosmin Lazar, Jonatan Taminau, Stijn Meganck, David Steenhoff, Alain Coletta, Colin Molter, Virginie de Schaetzen, Robin Duque, Hugues Bersini, and Ann Nowe. A survey on filter techniques for feature selection in gene expression microarray analysis. *IEEE/ACM transactions on computational biology and bioinformatics*, 9(4):1106–1119, 2012.
- Ismael Lemhadri, Feng Ruan, Louis Abraham, and Robert Tibshirani. Lassonet: A neural network with feature sparsity. *Journal of Machine Learning Research*, 22(127):1–29, 2021.
- Gen Li, Yuantao Gu, and Jie Ding. The efficacy of  $l_1$  regularization in two-layer neural networks. *arXiv preprint arXiv:2010.01048*, 2020.
- Jundong Li, Kewei Cheng, Suhang Wang, Fred Morstatter, Robert P Trevino, Jiliang Tang, and Huan Liu. Feature selection: A data perspective. *ACM Computing Surveys (CSUR)*, 50(6):94, 2018.

- Yifeng Li, Chih-Yu Chen, and Wyeth W Wasserman. Deep feature selection: theory and application to identify enhancers and promoters. *Journal of Computational Biology*, 23(5):322–336, 2016.
- Ofir Lindenbaum and Stefan Steinerberger. Randomly aggregated least squares for support recovery. *Signal Processing*, 180:107858, 2021.
- Ben J Marafino, W John Boscardin, and R Adams Dudley. Efficient and sparse feature selection for biomedical text classification via the elastic net: Application to icu risk stratification from nursing notes. *Journal of biomedical informatics*, 54:114–120, 2015.
- Michael L Metzker. Sequencing technologies—the next generation. *Nature reviews genetics*, 11(1):31, 2010.
- R Muthukrishnan and R Rohini. Lasso: A feature selection technique in predictive modeling for machine learning. In *2016 IEEE international conference on advances in computer applications (ICACA)*, pages 18–20. IEEE, 2016.
- Stephen O’Hara, Kun Wang, Richard A Slayden, Alan R Schenkel, Greg Huber, Corey S O’Hern, Mark D Shattuck, and Michael Kirby. Iterative feature removal yields highly discriminative pathways. *BMC genomics*, 14(1):1–15, 2013.
- Adam Paszke, Sam Gross, Soumith Chintala, Gregory Chanan, Edward Yang, Zachary DeVito, Zeming Lin, Alban Desmaison, Luca Antiga, and Adam Lerer. Automatic differentiation in pytorch. In *NIPS-W*, 2017.
- A C Pease, D Solas, E J Sullivan, M T Cronin, C P Holmes, and S P Fodor. Light-generated oligonucleotide arrays for rapid dna sequence analysis. *Proceedings of the National Academy of Sciences*, 91(11):5022–5026, 1994. ISSN 0027-8424. doi: 10.1073/pnas.91.11.5022. URL <https://www.pnas.org/content/91/11/5022>.
- Jason A Reuter, Damek V Spacek, and Michael P Snyder. High-throughput sequencing technologies. *Molecular cell*, 58(4):586–597, 2015.
- Debaditya Roy, K Sri Rama Murty, and C Krishna Mohan. Feature selection using deep neural networks. In *2015 International Joint Conference on Neural Networks (IJCNN)*, pages 1–6. IEEE, 2015.
- Simone Scardapane, Danilo Comminiello, Amir Hussain, and Aurelio Uncini. Group sparse regularization for deep neural networks. *Neurocomputing*, 241:81–89, 2017.
- Dari Shalon, Stephen J Smith, and Patrick O Brown. A dna microarray system for analyzing complex dna samples using two-color fluorescent probe hybridization. *Genome research*, 6(7):639–645, 1996.
- Li Shen, Sungeun Kim, Yuan Qi, Mark Inlow, Shanker Swaminathan, Kwangsik Nho, Jing Wan, Shannon L Risacher, Leslie M Shaw, John Q Trojanowski, et al. Identifying neuroimaging and proteomic biomarkers for mci and ad via the elastic net. In *International Workshop on Multimodal Brain Image Analysis*, pages 27–34. Springer, 2011.



- Dinesh Singh, Héctor Climente-González, Mathis Petrovich, Eiryo Kawakami, and Makoto Yamada. Fsnet: Feature selection network on high-dimensional biological data. *arXiv preprint arXiv:2001.08322*, 2020.
- Artem Sokolov, Daniel E Carlin, Evan O Paull, Robert Baertsch, and Joshua M Stuart. Pathway-based genomics prediction using generalized elastic net. *PLoS computational biology*, 12(3):e1004790, 2016.
- Aboozar Taherkhani, Georgina Cosma, and T Martin McGinnity. Deep-fs: A feature selection algorithm for deep boltzmann machines. *Neurocomputing*, 322:22–37, 2018.
- Robert Tibshirani. Regression shrinkage and selection via the lasso. *Journal of the Royal Statistical Society: Series B (Methodological)*, 58(1):267–288, 1996.
- Jorge R Vergara and Pablo A Estévez. A review of feature selection methods based on mutual information. *Neural computing and applications*, 24(1):175–186, 2014.
- Huiliang Xie and Jian Huang. Scad-penalized regression in high-dimensional partially linear models. *The Annals of Statistics*, 37(2):673–696, 2009.
- Yutaro Yamada, Ofir Lindenbaum, Sahand Negahban, and Yuval Kluger. Feature selection using stochastic gates. In *International Conference on Machine Learning*, pages 10648–10659. PMLR, 2020.
- Lei Yu and Huan Liu. Feature selection for high-dimensional data: A fast correlation-based filter solution. In *Proceedings of the 20th international conference on machine learning (ICML-03)*, pages 856–863, 2003.
- Hui Zou. The adaptive lasso and its oracle properties. *Journal of the American statistical association*, 101(476):1418–1429, 2006.
- Hui Zou and Trevor Hastie. Regularization and variable selection via the elastic net. *Journal of the royal statistical society: series B (statistical methodology)*, 67(2):301–320, 2005.

## Appendix A. Reproducibility

Table 6 shows the values of the hyperparameters that we use in our experiments. The tuning of these parameters is done in two ways: for low sample size biological data sets (first six data sets in the Table 6), we run five-fold cross-validation on a training partition. We split each of the remaining data sets into train, validation, and test ratio of 70:10:20 and used the validation set for tuning.

Dataset	Network topology	Activation	Learning Rate	$\lambda_1, \lambda_2$	$\mu_1, \mu_2$	Epoch
ALLAML	$d \rightarrow 250 \rightarrow d$	tanh	0.001	0.001,0.001	0.6,0.1	1050
GLIOMA	$d \rightarrow 250 \rightarrow d$	tanh	0.001	0.001,0.001	0.6,0.1	1050
SMK_CAN	$d \rightarrow 250 \rightarrow d$	tanh	0.001	0.001,0.001	0.6,0.1	1050
Prostate_GE	$d \rightarrow 250 \rightarrow d$	tanh	0.001	0.001,0.001	0.6,0.1	1050
GLL85	$d \rightarrow 250 \rightarrow d$	tanh	0.001	0.001,0.001	0.6,0.1	1050
CLL_SUB	$d \rightarrow 250 \rightarrow d$	tanh	0.001	0.001,0.001	0.6,0.1	1050
Mice Protein	$d \rightarrow 100 \rightarrow d$	tanh	0.008	0.001,0.001	0.2,0.6	1050
COIL20	$d \rightarrow 100 \rightarrow d$	tanh	0.008	0.001,0.001	0.8,0.1	1050
Isolet	$d \rightarrow 100 \rightarrow d$	tanh	0.008	0.001,0.001	0.8,0.3	1050
Human Activity	$d \rightarrow 100 \rightarrow d$	tanh	0.008	0.001,0.001	1.0,0.9	1050
MNIST	$d \rightarrow 100 \rightarrow d$	tanh	0.008	0.001,0.001	0.6,0.1	1050
FMNIST	$d \rightarrow 100 \rightarrow d$	tanh	0.008	0.001,0.001	0.6,0.1	1050

Table 6: Details of network topology and hyperparameters for SABCE. The number  $d$  is the input dimension of the network and is data set dependent.

## Appendix B. Compute Time

We present the average compute time of training for each data set in the table below.

Dataset	Training time (in minutes)
ALLAML	0.137
GLIOMA	0.122
SMK_CAN	0.889
Prostate_GE	0.121
GLI_85	0.809
CLL.SUB	0.276
Mice Protein	1.538
COIL20	2.563
Isolet	4.757
Human Activity	2.795
MNIST	20.621
FMNIST	23.697

Table 7: Average training time for Sparse Adaptive Bottleneck Centroid-Encoder for each data set.

### Appendix C. Sparsity Analysis of Stochastic Gates

In this section, we present a detailed analysis of the input feature sparsity of Stochastic Gates (STG)(Yamada et al., 2020). We have observed that STG performed competitively for the data sets with more samples than features (Table 5 of main paper); in contrast, the model performed relatively weakly on data sets where the number of variables is very large than the number of input data (Table 4 of main paper). Upon further investigation, it turns out that the model fails to induce feature sparsity on all six high-dimensional biological data sets. We fit the model on the training partition of each data set and then plot the probability of the stochastic gates in descending order, which we call the *sparsity plot*. We run STG using a wide range on  $\lambda$ , which controls the sparsity of the model.

In Figure 9, 10, 11, 12 and 13, we present the sparsity plot for Prostate\_GE, GLIOMA, SMK\_CAN, GLI\_85, and CLL.SUB data respectively. These sparsity plots are qualitatively similar to ALLAML (Figure 8), except for GLIOMA when  $\lambda = 5.0$ .

It is clear from this analysis that Stochastic Gate cannot sparsify the hi-dimensional biological data sets, and it's plausible that the model doesn't always pick the proper discriminatory feature set. The classification results in Table 4 (in the main article) do support the claim.

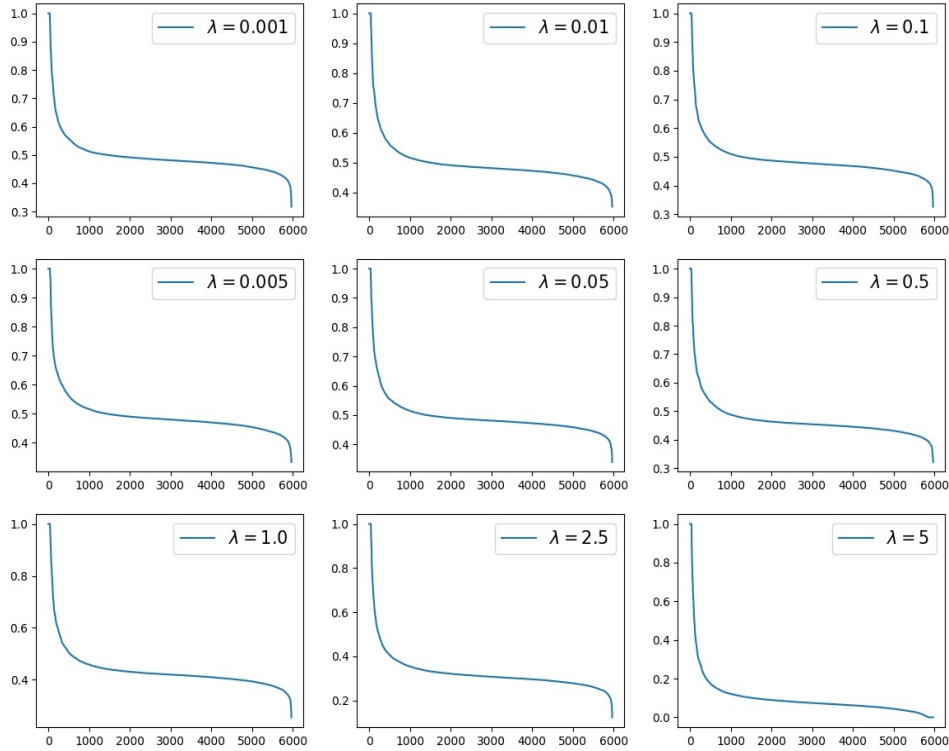


Figure 9: Sparsity analysis of Prostate\_GE data.

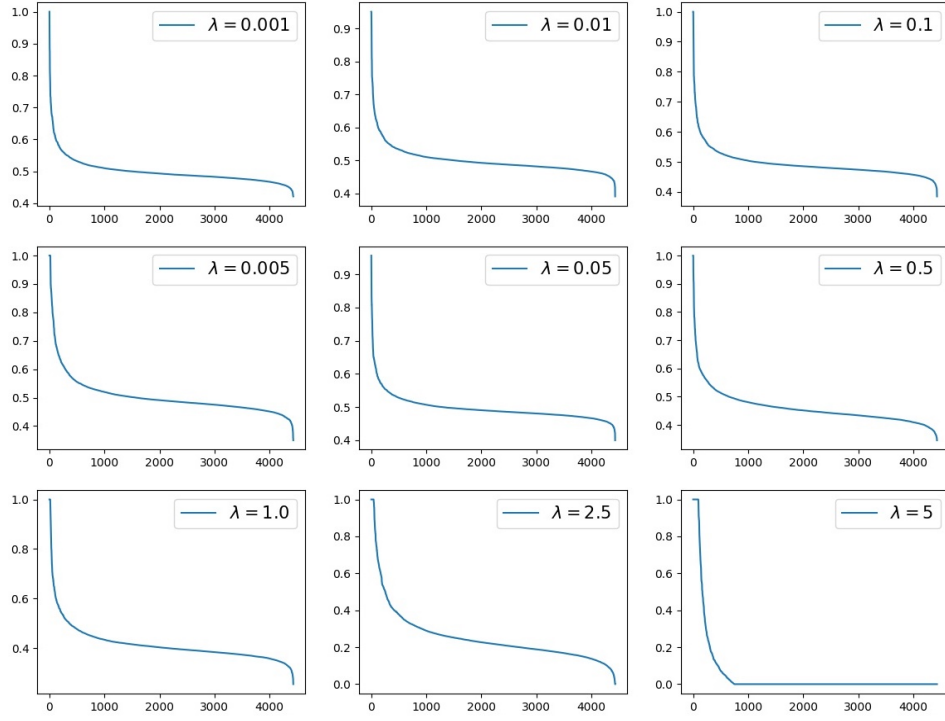


Figure 10: Sparsity analysis of GLIOMA data.

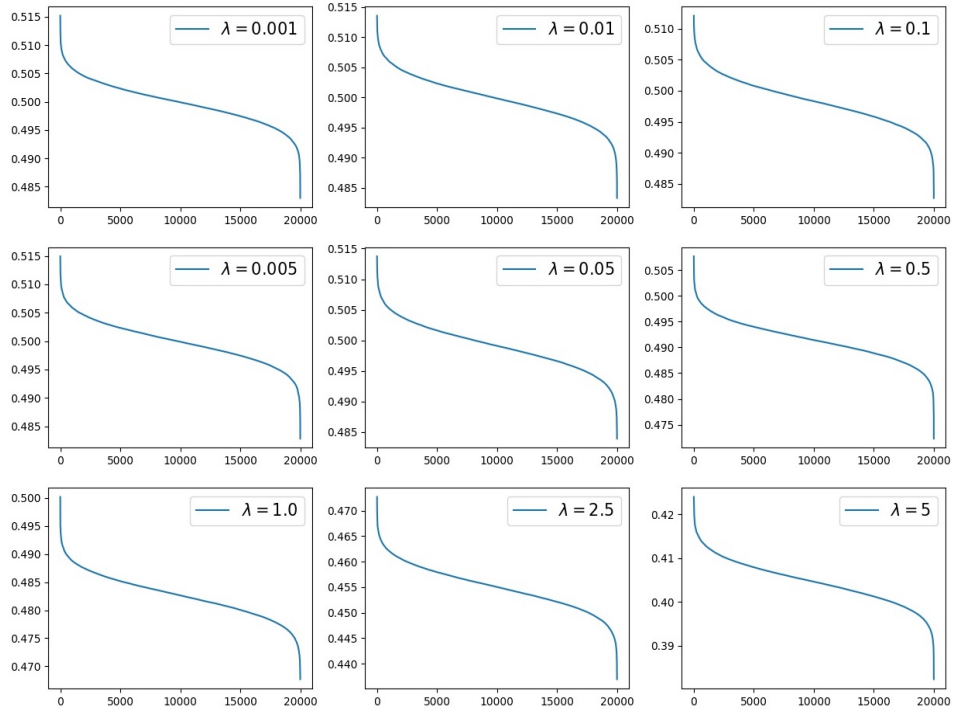


Figure 11: Sparsity analysis of SMK\_CAN data.

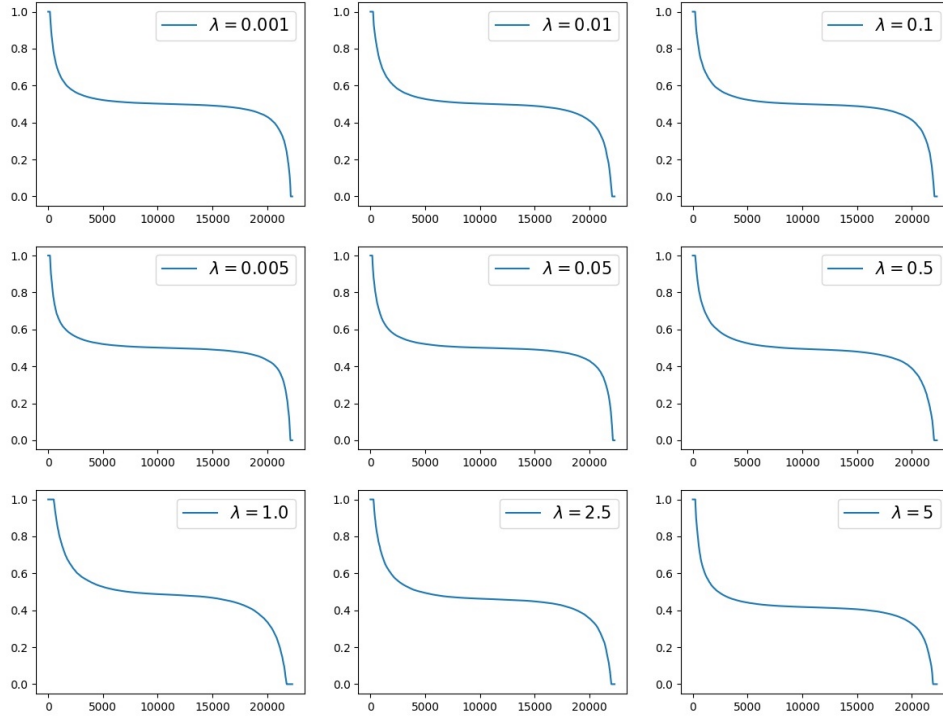


Figure 12: Sparsity analysis of GLL85 data.

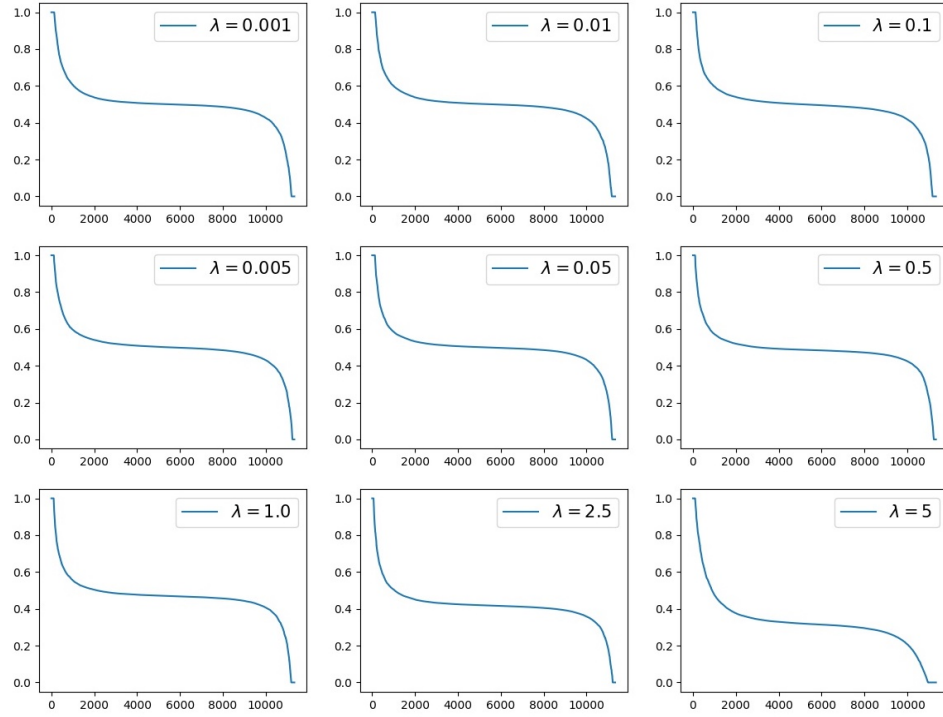


Figure 13: Sparsity analysis of CLL.SUB data.